Tumors Established with Cell Lines Selected for Oxaliplatin Resistance Respond to Oxaliplatin if Combined with Cetuximab

Marie Prewett,[1] Dhanvanthri S. Deevi,[1] Rajiv Bassi,[1] Fan Fan,[2] Lee M. Ellis,[2] Daniel J. Hicklin,[1] and James R. Tonra[1]

Abstract

Purpose: To establish whether cetuximab, a chimeric IgG1 antibody targeting epidermal growth factor receptor, has the potential to restore responsiveness to oxaliplatin in preclinical cancer models, as has been shown with irinotecan in irinotecan refractory metastatic colorectal cancer patients.

Experimental Design: The effects of cetuximab and oxaliplatin, alone or in combination, were tested *in vitro* and *in vivo* using human colorectal cancer cell lines selected for oxaliplatin resistance, as well as parental control cell lines. Evaluations were made of subcutaneous xenograft tumor growth in *nu/nu* athymic mice, as well as activation of mitogen-activated protein kinase (extracellular signal-regulated kinase 1/2) and AKT, expression of DNA repair genes, density of apurinic/apyrimidinic DNA damage, and accumulation of platinum-DNA adducts *in vitro*.

Results: Oxaliplatin + cetuximab efficacy in murine subcutaneous xenograft models was greater than that of monotherapies and independent of the responsiveness to oxaliplatin monotherapy. *In vitro*, cetuximab reduced expression of excision repair cross-complementation group 1 and XPF, which are key components of the nucleotide excision repair pathway involved in the excision of platinum-DNA adducts. In addition, cetuximab reduced expression of XRCC1, a component of the base excision repair pathway responsible for the repair of apurinic/apyrimidinic sites. Effects of cetuximab on DNA repair protein levels were downstream to effects on mitogen-activated protein kinase and AKT pathway activation. In line with effects on DNA repair protein expression, cetuximab increased the accumulation of platinum and apurinic/apyrimidinic sites on DNA during oxaliplatin treatment.

Conclusions: Cetuximab has the potential to salvage the benefits of oxaliplatin in oxaliplatin-resistant colorectal cancer patients by reducing DNA repair capacity.

Over 153,000 patients in the United States were diagnosed with colorectal cancer in 2007, and 52,000 deaths were attributed to this disease (1). Despite recent advances with targeted therapies and third-generation chemotherapies, response rates remain low and disease progression frequent. Targeted therapies being used for the treatment of colorectal cancer include inhibitors of vascular endothelial growth factor and epidermal growth factor receptor (EGFR; ref. 2). Cetuximab (ERBITUX), a chimeric IgG1 monoclonal antibody targeting EGFR, has been approved in the United States for patients with EGFR-expressing metastatic colorectal cancer. Cetuximab inhibition of EGFR activation affects tumor cell proliferation, cell survival pathways, and tumor cell invasion (3). Cetuximab may also inhibit cancer progression through antiangiogenic effects (4) and by inducing antibody-dependent cell cytotoxicity (5).

Cetuximab is approved for the treatment of colorectal cancer in patients that have failed irinotecan (CPT-11; CAMPTOSAR)–based therapies or who are intolerant to irinotecan-based therapies. In combination with irinotecan in patients who had failed an irinotecan-based regimen, the response rate was 23% for cetuximab + irinotecan compared with 11% for cetuximab monotherapy (6). The finding that the benefits of a cytotoxic therapy could be recovered in previously resistant patients through the use of cetuximab is an important concept also supported by preclinical studies (7).

Oxaliplatin (ELOXATIN) is a third-generation platinum agent with a broad spectrum of antitumor activity against a number of tumor types resistant to cisplatin, including colorectal cancer (8, 9). As with other platinum agents, oxaliplatin causes interstrand and intrastrand platinum-DNA adducts (9, 10). Platinum-DNA adducts inhibit gene transcription through sequestration of transcription factors (11) and are thought to lead to G_2-M arrest and apoptosis (12). The mechanism of cytotoxicity for platinum agents is however not

Authors' Affiliations: [1]Department of Preclinical Pharmacology, ImClone Systems Incorporated, New York, New York and [2]Departments of Surgical Oncology and Cancer Biology, University of Texas, M. D. Anderson Cancer Center, Houston, Texas
Received 7/18/07; revised 9/5/07; accepted 9/19/07.

The costs of publication of this article were defrayed in part by the payment of page charges. This article must therefore be hereby marked *advertisement* in accordance with 18 U.S.C. Section 1734 solely to indicate this fact.

Requests for reprints: Marie Prewett, ImClone Systems Incorporated, Department of Preclinical Pharmacology, 180 Varick Street, New York, NY 10014. Phone: 646-638-5018; Fax: 212-645-2054; E-mail: marie.prewett@imclone.com.

doi:10.1158/1078-0432.CCR-07-1768

firmly established (13), and 75% of cisplatin in cells is actually bound to proteins (12). Furthermore, both cisplatin and oxaliplatin increase reactive oxygen species (ROS) production (14, 15), resulting in protein, lipid, and DNA-based oxidation, with the latter forming apurinic/apyrimidinic sites among other types of DNA damage (14, 16).

Oxaliplatin is a component of first and second line combination therapies for the treatment of metastatic colorectal cancer (17). Despite efficacy in this indication, resistance to oxaliplatin-based therapies inevitably emerges with kinetics similar to those for earlier platinum agents (18). Oxaliplatin resistance mechanisms are similar, but not the same as for cisplatin (9), and include increased glutathione-mediated detoxification and increased DNA repair capacity (19). Cisplatin and oxaliplatin resistance overlap in their association with increased activity of the nucleotide excision repair (NER) protein, excision repair cross-complementation group 1 (ERCC1), which associates with XPF to cut the DNA platinum adducts at the 5′ end (20). In lung cancer patients, increased tumor ERCC1 mRNA is associated with a reduced response to cisplatin (21). Similarly, in colorectal cancer patients treated with 5-fluorouracil, cotreatment with oxaliplatin had greater effects in patients with an ERCC1 polymorphism resulting in reduced DNA repair activity (22).

Given the ability of EGFR signaling to regulate NER protein expression (23), cetuximab has the potential to restore the benefits of oxaliplatin therapy in colorectal cancer patients after the development of oxaliplatin resistance, similar to its role in combination with irinotecan. In preclinical colorectal cancer models, cetuximab increased the antitumor effects of oxaliplatin in the HCT-8 model, in which oxaliplatin was efficacious as a monotherapy, and in the HT-29 model, in which oxaliplatin monotherapy had no antitumor effect (24). No benefit of oxaliplatin + cetuximab was observed in HCT-116 and SW620 colorectal cancer models that also did not respond to oxaliplatin monotherapy. However, a submaximal oxaliplatin dosing regimen was used in this study (single dose of 10 mg/kg i.v.), making it difficult to conclusively assign an oxaliplatin resistance status to each model or to understand the full potential of combination treatment. Nor did this study evaluate the mechanism for the benefits of adding cetuximab to oxaliplatin, although reduced removal of platinum-DNA adducts in LoVo and HT-29 cells has been associated with *in vitro* synergism between a small molecule EGFR inhibitor, ZD1839, and oxaliplatin (25).

Although the above data support the addition of cetuximab to oxaliplatin-based therapy for colorectal cancer, they do not answer the question as to whether cetuximab can restore the benefits of oxaliplatin therapy in oxaliplatin-resistant tumor cells. Recently, variants of the KM-12 and HT-29 colorectal cancer cell lines have been developed by selecting for oxaliplatin resistance *in vitro* (26). We have evaluated antitumor effects of oxaliplatin + cetuximab in models established with these two lines, as well as in models established with parental HT-29 and KM-12 cells. Oxaliplatin sensitivity was determined *in vivo* using the maximum tolerated dose of oxaliplatin. In the models tested, the antitumor benefits of combination treatment with cetuximab and oxaliplatin were independent of oxaliplatin resistance. Moreover, the ability of oxaliplatin + cetuximab to achieve consistent and potent antitumor efficacy matched the ability of cetuximab to downregulate NER and base excision repair (BER) protein expression in tumor cells, resulting in increased accumulation of DNA damage.

Materials and Methods

Cell lines and reagents. Oxaliplatin-resistant HT29-OxR and KM12-OxR colorectal cancer cells, selected *in vitro* for resistance to the clinically relevant plasma concentration of 2 μmol/L oxaliplatin (26), were used. Parental control HT-29 cells were obtained from the American Type Culture Collection, and KM-12 cells were from the Division of Cancer Treatment and Diagnosis Tumor Repository of National Cancer Institute. Cells were maintained in McCoy's 5A media (HT29-OxR, HT-29) or RPMI 1640 (KM12-OxR, KM-12; Invitrogen) supplemented with 10% fetal bovine serum (HyClone) and 2 mmol/L GlutaMAX (Invitrogen), cultured at 37°C in a 5% CO_2 atmosphere, routinely passaged by Trypsin-EDTA (Invitrogen) treatment. Cetuximab was produced by ImClone Systems Incorporated. Oxaliplatin was obtained from LKT Laboratories and prepared in a solution of 5% USP dextrose. MEK1/2 inhibitor U0126 and phosphoinositide 3-kinase inhibitor LY294002 were obtained from CalBiochem.

Mice. Seven- to eight-week-old female athymic (*nu/nu*) mice were obtained from Charles River Laboratories. Mice were housed under pathogen-free conditions in microisolator cages with laboratory chow and water available *ad libitum*. All experiments and procedures were done in accordance with the U.S. Department of Agriculture, Department of Health and Human Services and NIH policies regarding the humane care and use of laboratory animals.

Fluorescence-activated cell sorting analysis. Subconfluent cultures, grown in 100 mm^2 plates, were washed in ice-cold PBS, and cells were detached by incubating monolayers in cell dissociation buffer (Sigma-Aldrich). Cells were washed twice with PBS containing 1% fetal bovine serum (flow buffer). Aliquots of 1×10^6 cells were incubated for 1 h on ice with primary antibody (cetuximab or buffer control) at 5 μg/mL in flow buffer. Cells were washed twice with flow buffer and then incubated for 30 min on ice with PE-labeled goat anti-human IgG Fc-specific secondary antibody (Jackson ImmunoResearch Laboratories, Inc.) diluted 1:200 in flow buffer. Cells were washed as above and resuspended in a minimal volume of flow buffer. Mean fluorescence intensity ratio was measured with a GUAVA EasyCyte flow cytometer (Guava Technologies).

Subcutaneous colorectal cancer xenograft testing. Colorectal cancer xenografts were established by injecting 5×10^6 tumor cells per mouse as described previously (7). Mice were randomized by tumor volume into treatment groups after the mean tumor volume reached ~200 mm^3. Mice were treated with USP saline MWF, cetuximab at 1 mg per dose (MWF), oxaliplatin (12 mg/kg, every 7 days), or a combination of cetuximab and oxaliplatin. All drug and antibody treatments were given by i.p. injection. Oxaliplatin dosing was started 1 day before the start of cetuximab dosing. Tumors were measured twice each week with calipers and tumor volumes calculated by the formula $[\pi / 6(w_1 \times w_2 \times w_2)]$, wherein w_1 represents the largest tumor diameter and w_2 represents the smallest tumor diameter. Treated versus control percentage (T/C%) was calculated as 100 × ratio of the relative tumor volumes in the experimental versus the control groups, with relative tumor volume = final tumor volume / initial tumor volume.

Western analysis. Cells were seeded at a density of 5×10^6 in 150 mm^2 tissue culture plates and cultured overnight in complete media. For the evaluation of the effects of cetuximab and oxaliplatin, cells were serum starved for 8 to 10 h and treated for 24 h with 10 μg/mL human IgG, 10 μg/mL cetuximab, and/or 1 μmol/L oxaliplatin. Cetuximab (10 μg/mL) is saturating for EGFR binding (not shown), and oxaliplatin (1 μmol/L) is close to the clinically relevant 2 μmol/L oxaliplatin concentration used to select the KM12-OxR and HT29-OxR cell lines. When evaluating the effects of U0126 and LY294002 (EMB Biosciences), cells were plated and starved overnight as above, followed

by treatment with 10 μmol/L U0126 or 10 μmol/L LY294002. After an hour of incubation, the cells were stimulated with 10 ng/mL EGF (Sigma) for 20 min at 37°C. At termination of the above studies, cultures were washed twice with ice cold PBS and cells were lysed with chilled radioimmunoprecipitation assay lysis buffer (1% Nonidet P-40, 0.5% sodium deoxycholate, 0.1% sodium dodecyl sulfate, 0.004% sodium azide; Santa Cruz Biotechnology) containing protease inhibitors. Lysates were centrifuged at 20,000×*g* for 15 min, and total protein concentration was estimated using bicinchoninic acid (Pierce). Twenty micrograms of cell lysates were reduced and resolved on 4% to 12% *bis*-Tris gels in 1× NuPAGE MES-SDS running buffer (Invitrogen). Resolved proteins were transferred to a nitrocellulose membrane using an iBLOT apparatus (Invitrogen). Membranes were blocked with 5% nonfat milk in TBS with Tween-20, 0.05% TBS-T on a rocker for 30 min. Blots were then incubated overnight at 4°C with primary antibodies against ERCC1, ERCC2, XPF (Abcam), pERK1/2, ERK1/2, pAKT, AKT (Cell Signaling), and β-actin (Sigma-Aldrich) at 1 to 2 μg/mL. After incubation, the membranes were washed with TBS-T and then incubated for 1 h at room temperature with species-specific, horseradish peroxidase–conjugated secondary antibodies (GE Healthcare Bio-Sciences). After washing in TBS-T, blots were briefly exposed to enhanced chemiluminescence Western blotting detection reagents (GE Healthcare Bio-Sciences), and chemiluminescence was detected with Kodak BioMax film (Kodak).

DNA damage assays. Cultured cells were treated for 48 h with either human IgG (control; 10 μg/mL), oxaliplatin (1 μmol/L), cetuximab (10 μg/mL), or a combination of oxaliplatin and cetuximab. Total cellular DNA from the cells was extracted using a DNeasy kit (Qiagen) as per manufacturer's instructions. The amount of DNA was quantified using a spectrophotometer (Nanodrop Technologies). Apurinic/apyrimidinic DNA site density was quantified using a colorimetric assay kit for DNA damage quantification from Oxford Biomedical Research, according to the manufacturer's instructions, using 5 μg total DNA per sample. The assay evaluates the number of apurinic/apyrimidinic sites on cellular DNA to serve as an indicator of DNA damage (27). The aldehyde reactive probe reacts specifically with exposed aldehyde on the open confirmation of apurinic/apyrimidinic sites in DNA. In this way, apurinic/apyrimidinic sites are tagged with biotinylated aldehyde reactive probe that is later detected with horseradish peroxidase–streptavidin. 3,3′,5,5′-Tetramethylbenzidine was used as a chromogen. 3,3′,5,5′-Tetramethylbenzidine reaction was stopped by the addition of 3M sulfuric acid, and color development was measured spectrophotometrically. For the quantification of platinum-DNA adducts, 100 μg genomic DNA was prepared from cultured cells for each experimental condition. The platinum content was then quantified using quadrupole inductively coupled plasma mass spectrometry. This analysis was done by Elemental Analysis, Inc., and results are reported in femtomole platinum per microgram DNA using oxaliplatin as the reference standard.

Statistical analysis. Statistical comparisons of tumor growth were calculated by RM ANOVA using JMP Statistical software (v. 5.1, SAS Institute). Statistical comparison for the effect of treatment on the degree of apurinic/apyrimidinic DNA site damage was made using a standard least squares method, with treatment and cell line as factors ($n = 3$). The correlations between T/C% and DNA damage measurements were evaluated by linear regression using the Pearson coefficient (r) to estimate the strength of significant relationships. All tests were two sided, with $P < 0.05$ indicating statistical significance.

Results

Cell surface EGFR expression. All four colorectal cancer cell lines used showed strong cell surface EGFR expression (mean fluorescence intensity ratio, ≥50; Fig. 1). The two lines selected for oxaliplatin resistance (HT29-OxR and KM12-OxR; Fig. 1B and D, respectively; ref. 26) expressed higher levels of cell surface EGFR than the two parental lines (HT-29 and KM-12; Fig. 1A and C, respectively). KM-12 cells exhibited a bimodal EGFR expression pattern.

Antitumor effects of oxaliplatin + cetuximab. The antitumor effects of cetuximab and oxaliplatin therapy, given alone or in combination, were evaluated in subcutaneous xenograft models established in *nu/nu* athymic mice with HT-29, HT29-OxR, KM-12, and KM12-OxR cells. Cetuximab was given at 1 mg/dose (~40 mg/kg) MWF, and oxaliplatin was dosed once per week at 12 mg/kg. The dose of oxaliplatin used is the maximum tolerated dose with this treatment schedule. Increasing the oxaliplatin dose to 18 mg/kg in the HT-29 xenograft model resulted in 13% body weight loss by day 25 of treatment and 60% lethality by day 29 of treatment, compared with 8% and 0%, respectively, for the 12 mg/kg dosing regimen.

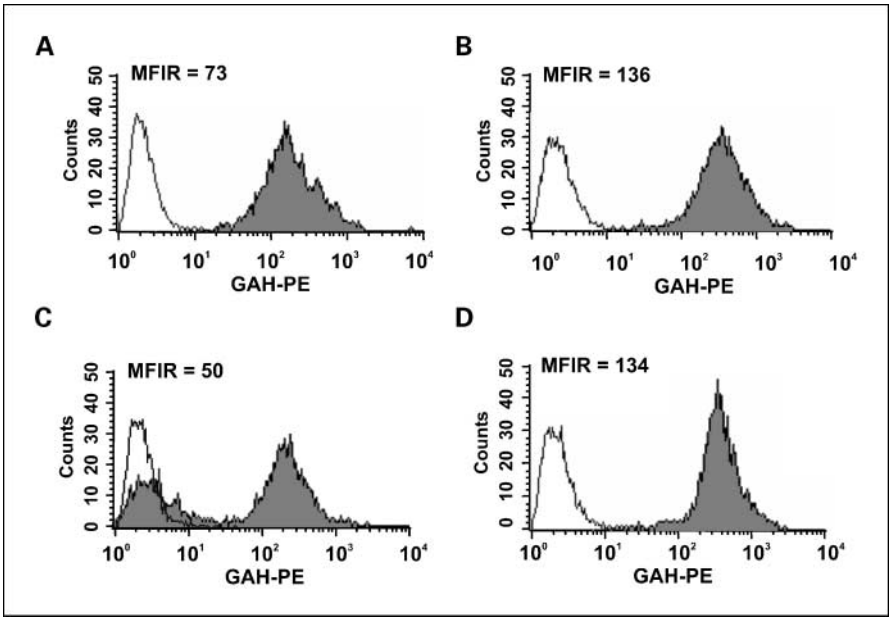

Fig. 1. Cell surface EGFR expression. EGFR expression by fluorescence-activated cell sorting analysis in HT-29 (*A*), HT29-OxR (*B*), KM-12 (*C*), and KM12-OxR (*D*) cells. Cells were incubated with cetuximab at 5 μg/mL, followed by a PE-conjugated antihuman IgG secondary antibody. Mean fluorescence intensity ratio (*MFIR*) is reported for cetuximab versus a negative staining control.

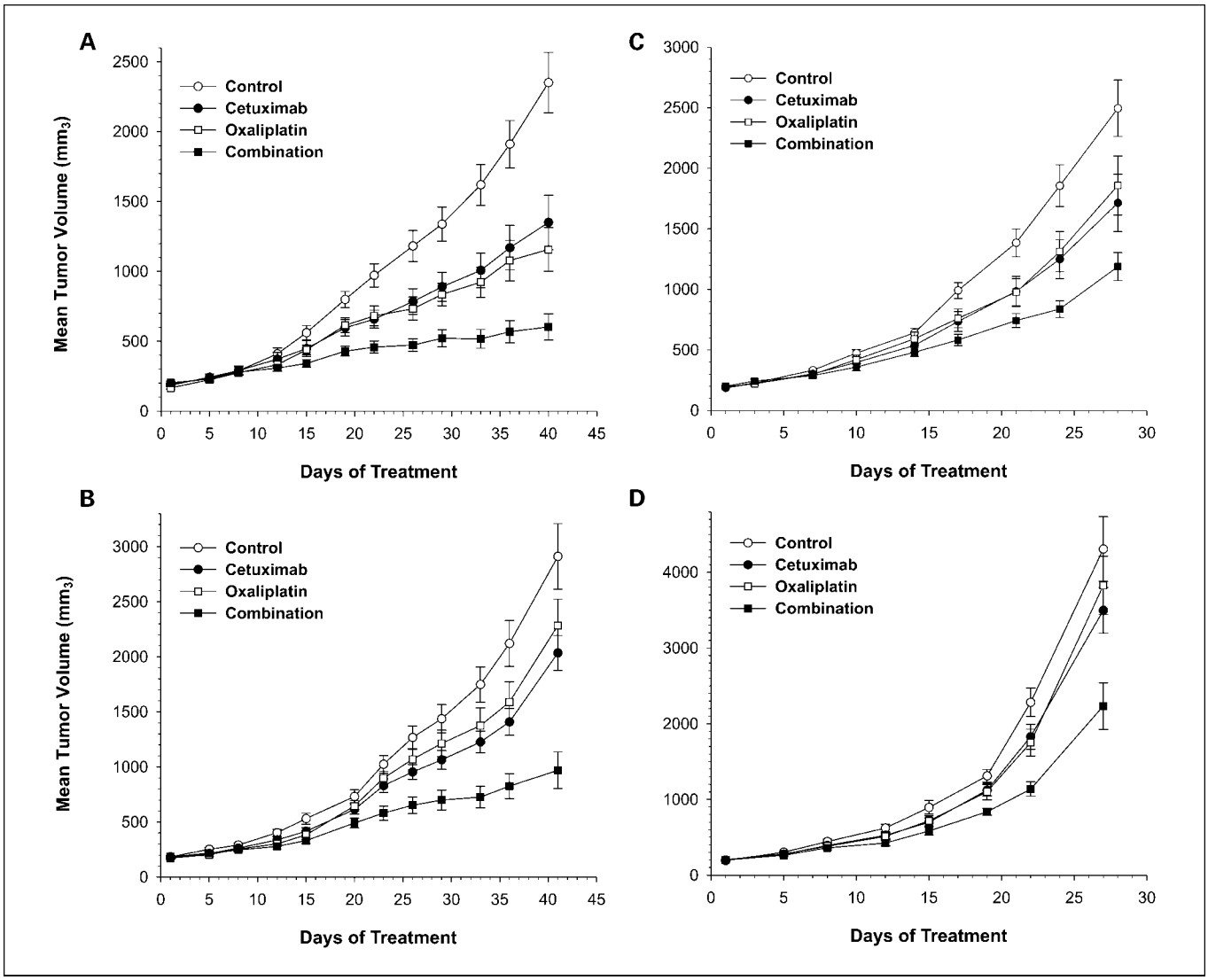

Fig. 2. Effects of oxaliplatin ± cetuximab in colorectal cancer xenograft models. HT-29 (*A*), HT29-OxR (*B*), KM-12 (*C*), and KM12-OxR (*D*) xenograft tumor volumes are plotted for controls (saline treated) and mice treated with cetuximab (1 mg per mouse, MWF), oxaliplatin (12 mg/kg, every 7 d) or the combination. Points, mean; bars, SEM. Values are for $n = 12$ per group.

HT-29 tumor growth was sensitive to both oxaliplatin and cetuximab (Fig. 2A; Table 1). Significantly greater antitumor effects were caused by the combination of these two agents in this model. HT29-OxR tumor growth in the control group was slightly more aggressive than that for HT-29 (Fig. 2B). Unlike HT-29, the growth of HT29-OxR tumors was resistant to oxaliplatin (Table 1). Cetuximab monotherapy again inhibited tumor growth, although to a lesser degree than in the HT-29 model (T/C% = 73% versus 59%). In spite of the resistance of the HT29-OxR tumor growth to oxaliplatin monotherapy, oxaliplatin was of significant benefit in this model if combined with cetuximab (Fig. 2B).

Cetuximab significantly inhibited the growth of KM-12 xenograft tumors, although the trend for an effect of oxaliplatin monotherapy (T/C% = 73%) did not reach statistical significance (Fig. 2C; Table 1). Oxaliplatin + cetuximab caused greater

Table 1. T/C% and RM ANOVA statistical comparisons for tumor growth

Treatment	HT-29		HT29-OxR		KM-12		KM12-OxR	
	T/C%	*P*	T/C%	*P*	T/C%	*P*	T/C%	*P*
Cetuximab versus control	59%	0.0008	73%	0.0127	71%	0.0239	78%	0.2856
Oxaliplatin versus control	57%	0.0001	84%	0.1455	73%	0.1168	84%	0.3924
Combination versus control	24%	<0.0001	33%	<0.0001	46%	0.0002	50%	0.0004
Combination versus cetuximab	—	0.0008	—	<0.0001	—	0.0339		0.0026
Combination versus oxaliplatin	—	0.0036	—	0.0002	—	0.0149		0.0031

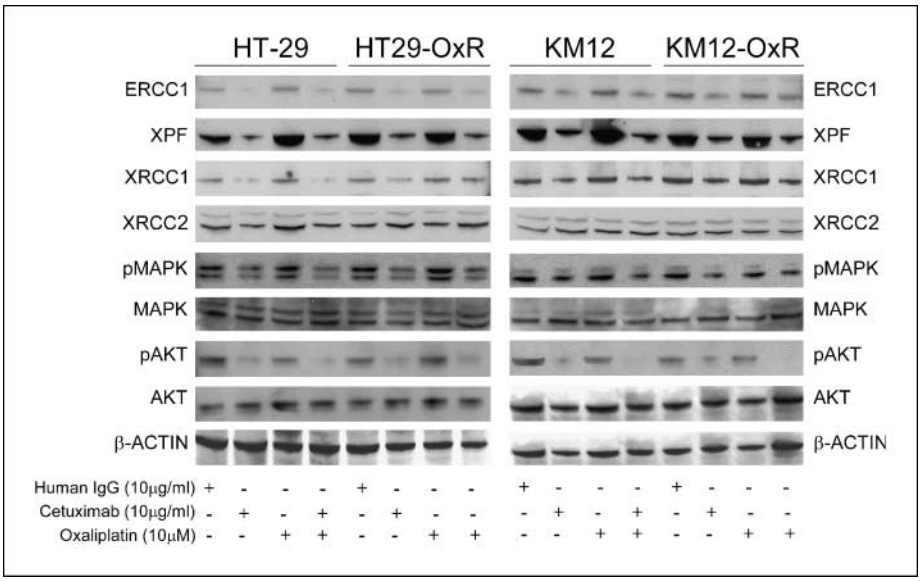

Fig. 3. Cetuximab reduces DNA repair protein expression. Effect of cetuximab (10 μg/mL) ± oxaliplatin (1 μmol/L) on the expression of ERCC1, XPF, and ERCC-2 by the indicated cell lines by Western analysis as described in Materials and Methods. The activation of AKT and MAPK was also evaluated, with β-actin used as a loading control.

KM12 tumor growth inhibition than either monotherapy. KM12-OxR tumor growth in the control group was more aggressive than that of KM-12 (Fig. 2D). The growth of KM12-OxR tumors was resistant to oxaliplatin (T/C% = 84%; Table 1), and cetuximab monotherapy did not significantly inhibit tumor growth. In spite of the resistance of KM12-OxR tumor growth to oxaliplatin monotherapy, oxaliplatin was of significant benefit in this model if combined with cetuximab (Fig. 2D).

Cetuximab decreases NER and BER protein expression. Platinum DNA adducts are removed through the NER process, reducing the toxicity of this class of agents. Increased NER activity has been supported as an important mechanism of resistance to platinum therapies (28). We therefore evaluated the ability of cetuximab to regulate NER proteins in our models. Cetuximab reduced the expression of ERCC1, as well as XPF in all four colorectal cancer cell lines (Fig. 3). Cetuximab reduced NER protein expression to the same extent, whether used alone or in combination with oxaliplatin. Although a trend for reduced expression of ERCC2/XPD was observed in HT-29, consistent effects of cetuximab on this NER protein were not observed, indicating the effects of cetuximab were specific to certain NER proteins. Cetuximab also lowered XRCC1 protein levels in both the oxaliplatin resistant and parental control colorectal cancer lines (Fig. 3). This indicates that cetuximab may also reduce BER because XRCC1 is a critical component of this DNA repair pathway (23).

Role for mitogen-activated protein kinase (ERK1/2) and AKT pathways in the regulation of DNA repair proteins. As in other models, cetuximab in the present study reduced the activation of the AKT cell survival pathway and the mitogen-activated protein kinase (MAPK) cell proliferation pathway (Fig. 3). EGF stimulation of MAPK has been implicated in ERCC1 regulation in prostate cancer models (23). To determine whether the AKT pathway or MAPK pathway was responsible for regulating ERCC1 in the present cell lines, we used small molecules to inhibit either AKT or MAPK activation during EGF stimulation of cells.

EGF stimulation of fasted cells activated AKT and MAPK in all cell lines tested and also increased the expression of DNA repair genes (Fig. 4). U0126 was used to inhibit the kinase that activates MAPK and MEK1/2 (29). LY294002 was used to inhibit phosphoinositide-3 kinase, which phosphorylates

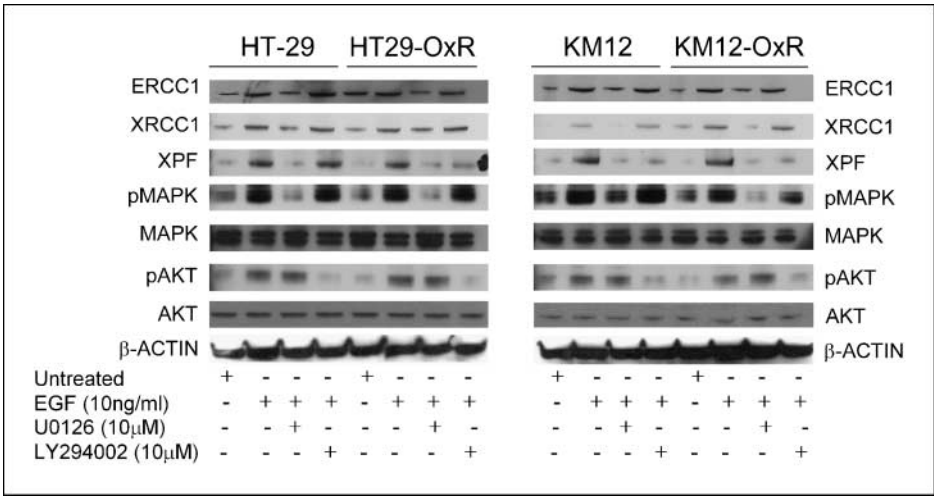

Fig. 4. Inhibition of MAPK activation, but not AKT activation, reduces ERCC1 in the presence of EGF. An inhibitor of MEK1/2 (U0126; 10 μmol/L) or phosphoinositide 3-kinase (LY294002; 10 μmol/L) was used to inhibit the activation of MAPK or AKT, respectively, in the presence of 10 ng/mL EGF. Western analysis of MAPK and AKT activation, as well as ERCC1 expression, was done as described in Materials and Methods.

phosphatidylinositol 4,5-bisphosphate to phosphatidylinositol 3,4,5-trisphosphate for recruiting AKT to the plasma membrane for activation through phosphorylation (30). Although LY294002 significantly inhibited EGF-induced AKT activation in all four cell lines, only inhibition of MAPK activation with U0126 was clearly associated with a consistent reduction in ERCC1 expression across all cell lines (Fig. 4). Moreover, inhibition of the MAPK pathway was also responsible for regulation of the BER protein XRCC1. In contrast to these pathways, XPF protein levels were regulated by activation of both the MAPK and AKT pathways in all cell lines except HT-29, wherein only the MAPK pathway was implicated.

Effects of cetuximab on oxaliplatin-induced DNA damage. As with other chemotherapeutic agents, oxaliplatin is thought to eventually kill tumor cells in part by increasing the production of ROS (14, 15). ROS produced in response to cisplatin treatment cause oxidative DNA damage associated with increased formation of apurinic/apyrimidinic sites (14, 31). Given the effects of cetuximab on the BER protein XRCC1 (Fig. 3) and the importance of BER to the repair of apurinic/apyrimidinic sites (32), we evaluated the effects of treatment on the density of DNA apurinic/apyrimidinic sites in our cell lines. Apurinic/apyrimidinic site density was increased by oxaliplatin and oxaliplatin + cetuximab treatment ($P < 0.0001$) but not by cetuximab monotherapy compared with controls, with mean $\pm$ SE values in each cell line (human IgG, cetuximab, oxaliplatin, cetuximab + oxaliplatin) of HT-29 (1.3 ± 0.3, 1.9 ± 0.6, 3.8 ± 0.2, 4.4 ± 0.9), HT29-OxR (1.2 ± 0.1, 0.8 ± 0.7, 1.9 ± 0.5, 4.6 ± 0.6), KM-12 (0.2 ± 0.7, 0.9 ± 0.5, 2.2 ± 0.5, 3.2 ± 0.7), and KM-12-OxR (1.2 ± 0.1, 1.1 ± 0.2, 2.7 ± 0.6, 3.4 ± 0.9). Cell line was a factor in determining apurinic/apyrimidinic site density only when evaluating the effect of oxaliplatin monotherapy ($P = 0.04$), likely due to the minimal effect of oxaliplatin monotherapy in HT29-OxR. Apurinic/apyrimidinic site formation in response to oxaliplatin was greater when it was combined with cetuximab compared with oxaliplatin alone ($P < 0.001$; Fig. 5A), independent of cell line. The importance of this effect is indicated by the significant correlation of apurinic/apyrimidinic site formation *in vitro* and antitumor efficacy with oxaliplatin-containing regimens ($r^2 = 0.75$, $P = 0.005$).

In line with effects on NER proteins described above, cetuximab also increased the accumulation of platinum-DNA adducts in response to oxaliplatin (Fig. 5B). The magnitude of platinum accumulation on DNA *in vitro* correlated significantly with the antitumor effects of oxaliplatin-containing dosing regimens *in vivo* ($r^2 = 0.81$, $P = 0.003$). Platinum was not detected in DNA samples collected from control or cetuximab-treated cells (not shown).

Discussion

In colorectal cancer patients, cetuximab restores the benefits of irinotecan (CPT-11) therapy in patients that had failed an irinotecan-based regimen (6). Colorectal cancer patients receiving oxaliplatin-based therapy may also not respond or eventually become resistant to this cytotoxic agent (18). Using preclinical colorectal cancer models, we have shown that even tumors established with cell lines selected for resistance to oxaliplatin can be induced to respond to this therapy if combined with cetuximab, a chimeric IgG1 antibody targeting EGFR. The consistent antitumor effects of oxaliplatin + cetuximab, independent of the sensitivity to oxaliplatin monotherapy, parallels the consistent ability of cetuximab to increase DNA damage caused by oxaliplatin associated with reduce expression of proteins involved in DNA damage repair.

Platinum-based therapies damage DNA through the formation of platinum-DNA adducts (33) and generation of ROS (14, 15). Oxaliplatin differs in activity from other platinum-based therapies in that it forms a bulky 1,2 diaminocyclohexane-Pt group in the DNA adduct. These 1,2 diaminocyclohexane-Pt adducts are poorly recognized by the DNA mismatch repair mechanism that contributes significantly to the cytotoxicity of cisplatin (9). Thus, the mechanisms of cell killing by oxaliplatin and cisplatin are not completely overlapping nor is their efficacy profile in different tumor models and types (9). Despite the broader activity of oxaliplatin in different tumor types, cells still emerge with resistance to oxaliplatin (19). Preclinically, resistance to oxaliplatin has been associated with functional changes, such as cellular transformation from proliferative to invasive phenotype (26), reduced drug accumulation (34), and increased expression of DNA polymerases (35). In the clinic, in contrast to evidence for differential mechanisms of cytotoxicity for cisplatin and oxaliplatin, these two agents share the fact that drug resistance or sensitivity has been associated with the

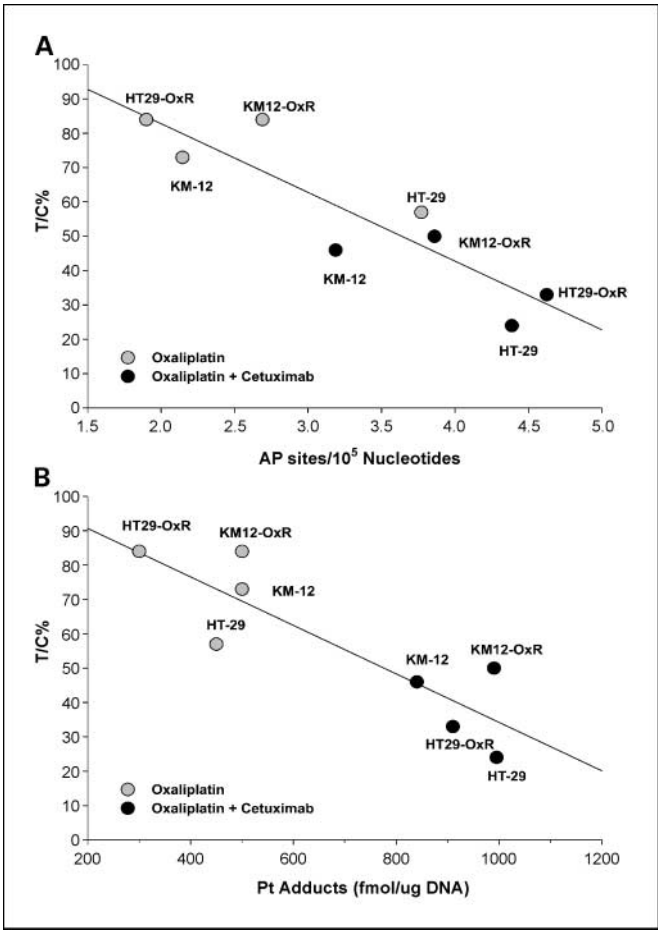

Fig. 5. *In vitro* DNA damage correlates with *in vivo* efficacy for oxaliplatin-containing regimens. *A,* points, mean of apurinic/apyrimidinic DNA site densities ($n = 3$ replicates in ELISA run) versus T/C% values from Table 1, for the oxaliplatin-containing regimens only. *B,* points, platinum accumulation on DNA versus T/C% values from Table 1, for the oxaliplatin-containing regimens only.

regulation of DNA damage repair components, particularly proteins involved in the NER pathway (Fig. 6; refs. 21, 36).

The NER pathway primarily repairs bulky lesions of transcribed genes induced by UV light, but also repairs oxidative lesions and platinum-DNA adducts (20, 37, 38). An XPA-RPA protein complex recognizes adducts and then interacts with a transcription factor complex that includes helicases ERCC2 and ERCC3 (XPD and XPB, respectively) that open the DNA. XPF and XPG are nucleases that form the remainder of this complex and cleave the DNA 5′ and 3′ to the adduct. More than any other component of the NER pathway, ERCC1 regulation has been associated with differences in the sensitivity to platinum agents. Increased activity of the NER protein ERCC1 has been established as a mechanism of resistance to cisplatin (36). Furthermore, reduced ERCC1 activity, through ERCC1 mutation (22) or reduced protein expression (39), is associated with an increased response to oxaliplatin in patients and in preclinical models. For this reason, it is important that cetuximab significantly lowered ERCC1 levels in all colorectal cancer cells evaluated, including two colorectal cancer cell lines selected to survive and proliferate in clinically relevant concentrations of oxaliplatin (2 μmol/L; ref. 26). At least in part through the reduction in ERCC1, as well as XPF, cetuximab was able to increase oxaliplatin-induced DNA damage in the form of platinum-DNA adducts.

Cetuximab achieved the down-regulation of ERCC1 through a reduction in MAPK activation. In agreement with this result, the expression of oncogenic H-Ras, upstream to MAPK activation in NIH-3T3 and MCF-7 human breast cancer cells, protects these cells against platinum agents through increased ERCC1 expression and increased DNA repair (39). Inhibition of AKT activation by cetuximab also contributed to reduced DNA repair potential through reduced expression of the NER protein XPF, which was also regulated by the MAPK pathway. In addition to reduced DNA repair, AKT inhibition could also contribute toward increased antitumor effects in combination with platinum agents (28), given the role of AKT in supporting the survival of tumor cells through inhibition of apoptosis in response to platinum-induced DNA damage (30).

We used *in vitro* techniques to evaluate the effects of cetuximab and oxaliplatin on DNA repair gene expression, AKT and MAPK activation, and DNA damage because of the greater control over experimental conditions and the resulting improvement in the ability to detect treatment effects on tumor cells relative to *in vivo* studies. Benefits of performing *in vitro* studies include the ability to maintain a relatively constant concentration of treatments surrounding tumor cells. More importantly, *in vitro* studies lack contaminating murine cell types, such as fibroblasts, endothelial cells, and immune cells that would decrease the ability of the current methods to conclusively establish effects of the human EGFR–specific

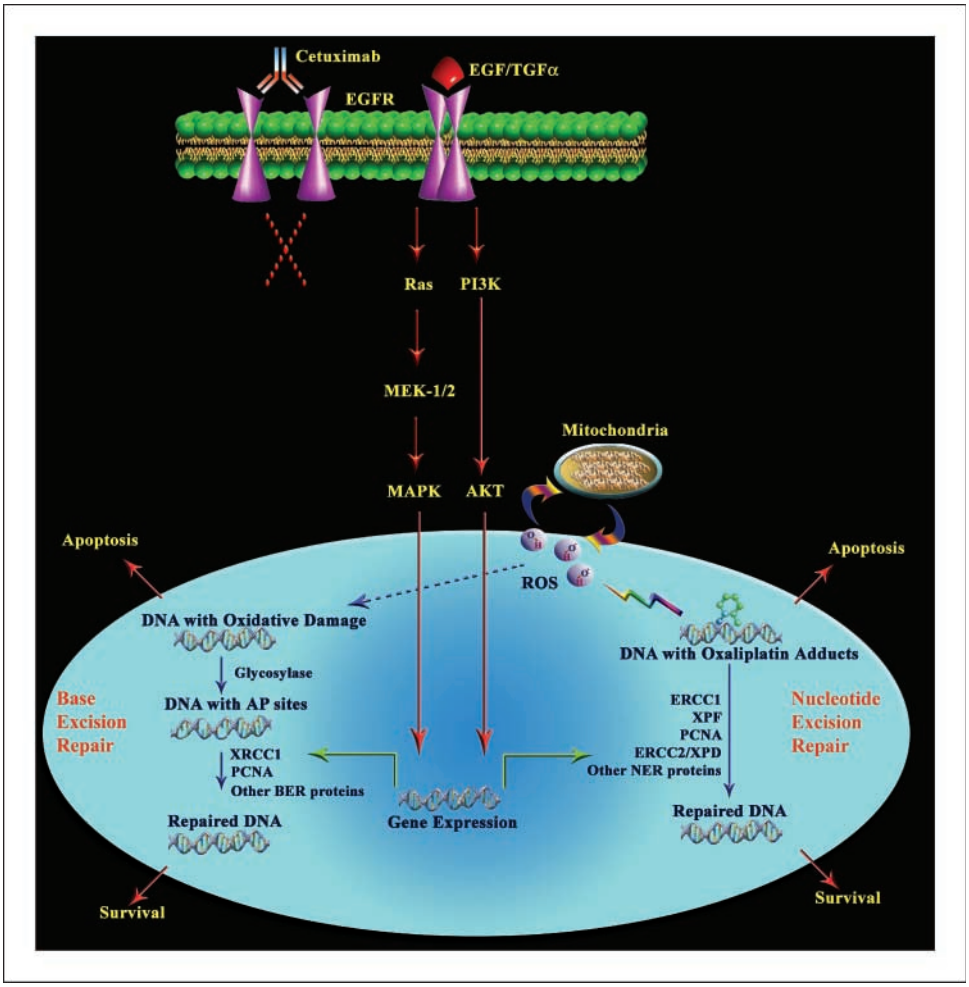

Fig. 6. Effects of EGFR signaling on NER and BER pathways responsible for repairing oxaliplatin-induced DNA damage.

antibody cetuximab on tumor cells growing as xenografts in mice. However, immunohistochemical techniques have been reported for evaluating platinum-adduct formation after cisplatin treatment in tissue sections (40); thus, in the future, these types of measurements may be used to extend our *in vitro* measurements to the *in vivo* situation. Nevertheless, our data show that the antitumor effects of oxaliplatin in the four tested colorectal cancer models were strongly correlated with the degree of oxaliplatin-induced DNA damage *in vitro*, damage in the form of platinum DNA-adducts as well as the less studied apurinic/apyrimidinic DNA damage.

Apurinic/apyrimidinic sites are continuously generated in DNA through hydrolysis of the *N*-glycosyl bond between DNA nucleotide sugar and base, which is a very labile bond compared with the phosphodiester bond in the DNA backbone (41). Apurinic/apyrimidinic sites can also be generated by glycosylase enzymes that remove oxidative, chemical, or radiation-damaged bases as part of the BER process (14, 42). Cisplatin causes apurinic/apyrimidinic sites in association with increased oxidative DNA damage in rat kidneys, evaluated by measuring 8-oxoguanine levels (14). Apurinic/apyrimidinic site and 8-oxoguanine accumulation are markers for oxidative damage (31); thus, ROS production induced by cisplatin is thought to underlie the measured increase in apurinic/apyrimidinic sites. Cisplatin ROS production occurs directly after its interaction with DNA in a cell-free system (43). Moreover, ROS generated in response to cisplatin can cause the loss of mitochondrial membrane potential (14), resulting in increased ROS production by mitochondria (44) establishing a positive feedback loop for ROS production. Similar to results with cisplatin, oxaliplatin has been shown to significantly increase oxygen radical production by murine CT-26 colorectal cancer cells (15), and therefore, increased ROS production is likely to contribute toward the observed increase in apurinic/apyrimidinic sites with oxaliplatin treatment in colorectal cancer cell lines (Fig. 6).

The finding that the ability of oxaliplatin to induce apurinic/apyrimidinic sites was increased with cetuximab indicates that the BER pathway, responsible for repairing this type of DNA damage (32, 38), is also inhibited by cetuximab through effects beyond ERCC1 and XPF. This possibility is in line with a report of increased expression of XRCC1, a BER scaffold protein (38), in response to EGF stimulation of prostate cancer cells (23) and the demonstration of reduced XRCC1 expression with cetuximab treatment in the present study, downstream to inhibition of signaling in the MAPK pathway. Further support for the potential importance of the EGFR pathway in BER is derived from the finding that tyrosine phosphorylation of proliferating cell nuclear antigen by activated EGFR is important for its normal functioning (45). Proliferating cell nuclear antigen is an important component of many DNA repair processes, including both NER and BER (Fig. 6; ref. 38). Therefore, the inhibition of EGFR with cetuximab decreases the capacity to repair multiple types of oxaliplatin-induced DNA damage by inhibiting multiple DNA repair pathways.

It should be noted that inhibition of the NER pathway, through reduction of ERCC1 and XPF protein levels, could also contribute to an increase in apurinic/apyrimidinic sites when oxaliplatin is combined with cetuximab. Extrapolating from results with cisplatin (43, 44), ROS generated in response to oxaliplatin is expected to cause oxidative DNA damage, including 8-oxoguanine lesions, associated with increased apurinic/apyrimidinic sites (31), presumably because of the inability to remove all of the apurinic/apyrimidinic sites generated by glycosylase cleavage of ROS-damaged bases. NER deficiency due to cetuximab-induced ERCC1 and XPF protein down-regulation may drive increased ROS production resulting from the oxaliplatin-DNA interaction, followed by increased activity in the positive feedback loop for ROS production with the mitochondria. Increased ROS production in this NER-deficient state induced by cetuximab would then result in a further increase in apurinic/apyrimidinic sites. Moreover, the reduction in the potential contribution of the NER pathway to remove bases in transcribed DNA with oxidative damage (37) could further increase the accumulation of oxidative DNA damage and apurinic/apyrimidinic sites. In support of this last point, *ERCC1* null mice show increased accumulation of oxidative DNA damage in the liver, evaluated by measuring the level of 8-oxoguanine (46). *ERCC1* transgene expression in the liver eliminated the accumulation of this oxidative DNA damage.

In conclusion, cetuximab restores the utility of irinotecan in irinotecan refractory colorectal cancer, both in preclinical models (7) and in the clinic (6). In the present study, the increased antitumor effects of oxaliplatin + cetuximab, as well as the indicators of reduced NER and BER DNA repair capacity and increased DNA damage, were independent of whether the cell lines used were selected for oxaliplatin resistance. Thus, similar to the case with irinotecan, oxaliplatin-resistant colorectal cancer patients may still benefit from oxaliplatin therapy if given in combination with cetuximab.

Acknowledgments

We thank Maxine Melchior and Dipa Patel at ImClone Systems Incorporated, for their technical support.

References

1. Jemal A, Siegal R, Ward E, et al. Cancer Statistics, 2007. CA Cancer J Clin 2007;57:43–66.
2. Chung KY, Saltz LB. Antibody-based therapies for colorectal cancer. Oncologist 2005;10:701–9.
3. Mendelsohn J, Baselga J. Status of epidermal growth factor receptor antagonists in the biology and treatment of cancer. J Clin Oncol 2003;21:2787–99.
4. Perrotte P, MatsumotoT, Inoue K, et al. Anti-epidermal growth factor receptor antibody C225 inhibits angiogenesis in human transitional cell carcinoma growing orthotopically in nude mice. Clin Cancer Res 1999;5:257–65.
5. Kawaguchi Y, Kono K, Mimura K, Sugai H, Akaike H, Fujii H. Cetuximab induce antibody-dependent cellular cytotoxicity against EGFR-expressing esophageal squamous cell carcinoma. Int J Cancer 2007;120:781–7.
6. Cunningham D, Humblet Y, Siena S, et al. Cetuximab monotherapy and cetuximab plus irinotecan in irinotecan-refractory metastatic colorectal cancer. N Engl J Med 2004;351:337–45.
7. Prewett MC, Hooper AT, Bassi R, Ellis LM, Waksal HW, Hicklin DJ. Receptor Monoclonal Antibody IMC-C225 in Combination with Irinotecan (CPT-11) against Human Colorectal Tumor Xenografts. Clin Cancer Res 2002;8:994–1003.
8. Vaisman A, Chaney SG. The efficiency and fidelity of translesion synthesis past cisplatin and oxaliplatin GpG adducts by human DNA polymerase β. J Biol Chem 2000;275:13017–25.
9. Raymond E, Faivre S, Chaney S, Woynarowski J, Cvitkovic E. Cellular and molecular pharmacology of oxaliplatin. Mol CancerTher 2002;1:227–35.
10. Woynarowski JM, Faivre S, Herzig MC, et al. Oxaliplatin-induced damage of cellular DNA. Mol Pharmacol 2000;58:920–7.

11. Jordan P, Carmo-Fonseca M. Molecular mechanisms involved in cisplatin cytotoxicity. Cell Mol Life Sci 2000;57:1229–35.

12. Fujie Y, Yamamoto H, Ngan CY, et al. Oxaliplatin, a potent inhibitor of survivin, enhances paclitaxel-induced apoptosis and mitotic catastrophe in colon cancer cells. Jpn J Clin Oncol 2005;35:453–63.

13. Gonzalez VM, Fuertes MA, Alonso C, Perez JM. Is cisplatin-induced cell death always produced by apoptosis? Mol Pharmacol 2001;59:657–63.

14. Satoh M, Kashihara N, Fujimoto S, et al. A novel free radical scavenger, edarabone, protects against cisplatin-induced acute renal damage *in vitro* and *in vivo*. J Pharmacol Exp Ther 2003;305:1183–90.

15. Laurent A, Nicco C, Chereau C, et al. Controlling tumor growth by modulating endogenous production of reactive oxygen species. Cancer Res 2005; 65:948–56.

16. Ramana CV, Boldogh I, Izumi T, Mitra S. Activation of apurinic/apyrimidinic endonuclease in human cells by reactive oxygen species and its correlation with their adaptive response to genotoxicity of free radicals. Proc Natl Acad Sci U S A 1998;95:5061–6.

17. Colucci G, Gebbia V, Paoletti G, et al. Phase III randomized trial of FOLFIRI versus FOLFOX in the treatment of advanced colorectal cancer: a multicenter study of the Gruppo Oncologico Dell'Italia Meridionale. J Clin Oncol 2005;23:4866–75.

18. Mishima M, Samimi G, Kondo A, Lin X, Howell SB. The cellular pharmacology of oxaliplatin resistance. Eur J Cancer 2002;38:1405–12.

19. Hector S, Bolanowska-Higdon W, Zdanowicz J, Hitt S, Pendyala L. *In vitro* studies on the mechanisms of oxaliplatin resistance. Cancer Chemother Pharmacol 2001;48:398–406.

20. Wood RD. Nucleotide excision repair in mammalian cells. J Biol Chem 1997;272:23465–8.

21. Rosell R, Taron M, Barnadas A, Scagliotti G, Sarries C, Roig B. Nucleotide excision repair pathways involved in cisplatin resistance in non-small-cell lung cancer. Cancer Control 2003;10:297–305.

22. Viguier J, Boige V, Miquel C, et al. ERCC1 codon 118 polymorphism is a predictive factor for the tumor response to oxaliplatin/5-fluorouracil combination chemotherapy in patients with advanced colorectal cancer. Clin Cancer Res 2005;11:6212–7.

23. Yacoub A, McKinstry R, Hinman D, Chung T, Dent P, Hagan MP. Epidermal growth factor and ionizing radiation up-regulate the DNA repair genes XRCC1 and ERCC1 in DU145 and LNCaP prostate carcinoma through MAPK signaling. Radiat Res 2003;159: 439–52.

24. Balin-Gauthier D, Delord JP, Rochaix P, et al. *In vivo* and *in vitro* antitumor activity of oxaliplatin in combination with cetuximab in human colorectal tumor cell lines expressing different level of EGFR. Cancer Chemother Pharmacol 2006;57:709–18.

25. Xu JM, Azzariti A, Severino M, Lu B, Colucci G, Paradiso A. Characterization of sequence-dependent synergy between ZD1839 ("Iressa") and oxaliplatin. Biochem Pharmacol 2003;66:551–63.

26. Yang AD, Fan F, Camp ER, et al. Chronic oxaliplatin resistance induces epithelial-to-mesenchymal transition in colorectal cancer cell lines. Clin Cancer Res 2006;12:4147–53.

27. Kubo K, Ide H, Wallace SS, Kow YW. A novel, sensitive, and specific assay for abasic sites, the most commonly produced DNA lesion. Biochemistry 1992; 31:3703–8.

28. Siddik ZH. Cisplatin: mode of cytotoxic action and molecular basis of resistance. Oncogene 2003;22: 7265–79.

29. Zhang W, Liu HT. MAPK signal pathways in the regulation of cell proliferation in mammalian cells. Cell Res 2002;12:9–18.

30. Song G, Ouyang G, Bao S. The activation of Akt/PKB signaling pathway and cell survival. J Cell Mol Med 2005;9:59–71.

31. Lu AL, Li X, Gu Y, Wright PM, Chang DY. Repair of oxidative DNA damage: mechanisms and functions. Cell Biochem Biophys 2001;35:141–70.

32. Vidal AE, Boiteux S, Hickson ID, Radicella JP. XRCC1 coordinates the initial and late stages of DNA abasic site repair through protein-protein interactions. EMBO J 2001;20:6530–9.

33. Scheeff ED, Briggs JM, Howell SB. Molecular modeling of the intrastrand guanine-guanine DNA adducts produced by cisplatin and oxaliplatin. Mol Pharmacol 1999;56:633–43.

34. Plasencia C, Martinez-Balibrea E, Martinez-Cardus A, Quinn DI, Abad A, Neamati N. Expression analysis of genes involved in oxaliplatin response and development of oxaliplatin-resistant HT-29 colon cancer cells. Int J Oncol 2006;29:225–35.

35. Vaisman A, Warren MW, Chaney SG. The effect of DNA structure on the catalytic efficiency and fidelity of human DNA polymerase β on templates with platinum-DNA adducts. J Biol Chem 2001; 276:18999–9005.

36. Olaussen KA, Dunant A, Fouret P, et al. DNA repair by ERCC1 in non-small-cell lung cancer and cisplatin-based adjuvant chemotherapy. N Engl J Med 2006; 355:983–91.

37. Le Page F, Klungland A, Barnes DE, Sarasin A, Boiteux S. Transcription coupled repair of 8-oxoguanine in murine cells: the ogg1 protein is required for repair in nontranscribed sequences but not in transcribed sequences. Proc Natl Acad Sci U S A 2000; 97:8397–402.

38. Hansen WK, Kelley MR. Review of mammalian DNA repair and translational implications. J Pharmacol Exp Ther 2000;295:1–9.

39. Youn CK, Kim MH, Cho HJ, et al. Oncogenic H-Ras up-regulates expression of ERCC1 to protect cells from platinum-based anticancer agents. Cancer Res 2004;64:4849–57.

40. Liedert B, Pluim D, Schellens J, Thomale J. Adduct-specific monoclonal antibodies for the measurement of cisplatin-induced DNA lesions in individual cell nuclei. Nucleic Acids Res 2006;34:e47.

41. Lindahl T. Instability and decay of the primary structure of DNA. Nature 1993;362:709–15.

42. Beger RD, Bolton PH. Structures of apurinic and apyrimidinic sites in duplex DNAs. J Biol Chem 1998; 273:15565–73.

43. Masuda H, Tanaka T, Takahama U. Cisplatin generates superoxide anion by interaction with DNA in a cell-free system. Biochem Biophys Res Commun 1994;203:1175–80.

44. Kruidering M, Van de Water B, de Heer E, Mulder GJ, Nagelkerke JF. Cisplatin-induced nephrotoxicity in porcine proximal tubular cells: mitochondrial dysfunction by inhibition of complexes I to IV of the respiratory chain. J Pharmacol Exp Ther 1997;280:638–49.

45. Wang SC, Nakajima Y, Yu YL, et al. Tyrosine phosphorylation controls PCNA function through protein stability. Nat Cell Biol 2006;8:1359–68.

46. Selfridge J, Hsia KT, Redhead NJ, Melton DW. Correction of liver dysfunction in DNA repair-deficient mice with an ERCC1 transgene. Nucleic Acids Res 2001;29:4541–50.